Available online at www.sciencedirect.com
ScienceDirect
Journal of Power Sources 174 (2007) 932–937
JOURNAL OF POWER SOURCES
www.elsevier.com/locate/jpowsour

Short communication

Synthesis of hollandite-type $Li_yMn_{1-x}Co_xO_2$ ($x = 0$–0.15) by Li^+ ion-exchange in molten salt and the electrochemical property for rechargeable lithium battery electrodes

Naoaki Kumagai [a,*], Satoru Oshitari [a], Shinichi Komaba [b], Yoshihiro Kadoma [a]

[a] *Department of Frontier Materials and Functional Engineering, Graduate School of Engineering, Iwate University, 4-3-5, Morioka 020-8551, Japan*
[b] *Tokyo University of Science, 1-3 Kagurazaka, Shinjuku, Tokyo 162-8601, Japan*

Available online 3 July 2007

Abstract

The Li^+ ion-exchange reaction of K^+-type α-$K_{0.14}MnO_{1.93}\cdot 0.18H_2O$ and its Co-doped α-$K_{0.14}(Mn_{0.85}Co_{0.15})O_{1.96}\cdot 0.21H_2O$ with a large (2 × 2) tunnel structure has been investigated in a $LiNO_3$/LiCl molten salt at 300 °C. The Li^+ ion-exchanged products were examined by chemical analysis, X-ray diffraction, and scanning and transmission electron microscopic measurements. Almost all the K^+ ions and the hydrogens of water molecules in the (2 × 2) tunnel of α-MnO_2 and its Co-doped one were exchanged by Li^+ ions in the molten salt, resulting in Li^+-type α-MnO_2 and its Co-doped one containing Li^+ ions as well as Li_2O (lithium oxide) in the (2 × 2) tunnel with maintaining the original hollandite structure.

The electrochemical properties including charge–discharge cycling of the Li^+ ion-exchanged α-MnO_2 and its Co-doped samples have been investigated as insertion compounds in the search for new cathode materials for rechargeable lithium batteries. The Li^+ ion-exchanged α-MnO_2 and its Co-doped samples provided higher capacities than the K^+-type parent materials on initial discharge and charge–discharge cyclings, probably due to the structural stabilization with the existence of Li_2O in the (2 × 2) tunnels.

Keywords: Hollandite manganese oxide; Li^+ ion-exchange in the molten salt; Lithium batteries; Charge–discharge properties

1. Introduction

Manganese oxides are most attractive as cathodes for rechargeable lithium batteries from environmental and economic standpoints [1–3]. Manganese oxides occur in many structural forms, such as α-, β-, γ-, birnessite-, and todorokite-MnO_2. Among various modifications of MnO_2, hollandite-type α-MnO_2 has the tetragonal crystal system with a (2 × 2) tunnel structure containing water molecules and alkaline cations (barium, potassium etc.) in the large tunnel. The hollandite-type MnO_2 is prepared conventionally by precipitation from Mn(II) solution with an oxidizing agent, such as $KMnO_4$, $K_2S_2O_8$, or their sodium or ammonium salt [4,5]. The MnO_2 prepared by this method contains K^+, NH_4^+, or Ba^{2+} ion in the (2 × 2) tunnel. However, these cations would block Li^+ ion transport through the (2 × 2) tunnel. Tsuji and Abe [6] have reported that the cations can be extracted from the tunnel by treating with concentrated HNO_3, but the complete extraction is very difficult, because K^+ or NH_4^+ ions are tightly fixed in the (2 × 2) tunnel. Feng et al. [7] have synthesized H^+-type α-MnO_2 without foreign metal cations (K^+, NH_4^+, Ba^{2+}) in the (2 × 2) tunnel directly by reacting $LiMnO_4$ with $Mn(NO_3)_2$ in an H_2SO_4 acidic solution and showed that the H^+-type α-MnO_2 gives a rechargeable capacity of about 150 mAh g^{-1} at the 10th cycle. Botkovitz et al. [8] have prepared a hollandite-type Li_xMnO_2 by the solid-state reaction between $NH_4Mn_8O_{16}$ and $LiOH\cdot H_2O$ at 300–400 °C and have examined the structural and electrochemical characteristics. Johnson et al. [9,10] have reported that the reaction of α-MnO_2 with LiOH at 275 °C results in lithia-stabilized products $xLi_2O\cdot MnO_2$ ($0 < x < 0.15$) in which Li_2O molecules substitute for the H_2O molecules in hydrated α-MnO_2. These lithia-stabilized α-MnO_2 electrodes provide a rechargeable capacity of about 150 mAh g^{-1} at the 10th cycle in lithium cell.

In our previous works [11,12], we have investigated the synthesis and characterization of K^+-type α-$Mn_xM_{1-x}O_2$, where a transition metal, such as M = Co or Fe is substituted for the Mn, and furthermore, examined the electrochemical character-

* Corresponding author. Tel.: +81 19 621 6328; fax: +81 19 621 6328.
E-mail address: nkumagai@iwate-u.ac.jp (N. Kumagai).

0378-7753/$ – see front matter © 2007 Elsevier B.V. All rights reserved.
doi:10.1016/j.jpowsour.2007.06.221

istics including charge–discharge cyclings of the metal-doped α-MnO_2 as cathodes for rechargeable lithium batteries. In this work, we will report the preparation of Li^+-type hollandite and its Co-doped α-MnO_2 samples by ion-exchanging the K^+-type α-MnO_2 in the Li^+ ion-containing molten salt at 300 °C and their electrochemical performances for rechargeable lithium battery cathodes.

2. Experimental

α-$K_{0.14}MnO_2{\cdot}0.18H_2O$ (denoted as K-Hol), and its Co-doped α-$K_{0.14}(Mn_{0.85}Co_{0.15})O_2{\cdot}0.21H_2O$ (Co-K-Hol) samples were prepared by the solution technique as described in our previous paper [11], as follows. Aqueous solutions consisting of 1 M $MnSO_4$ and 1 M $CoSO_4$ solutions were added to a constantly stirred 1 M $K_2S_2O_8$ aqueous solution at 80 °C, and the mixed solution was further stirred for 7 h at 80 °C. The precipitate was filtered, washed with water, and dried in an oven at 80 °C for about 12 h. To synthesize the Li^+-type hollandite MnO_2 samples and its Co-doped samples, the prepared K^+-type K-Hol and Co-K-Hol samples were mixed with $LiNO_3$/LiCl (=88:12) in a porcelain crucible at a ratio of Li/K = 5 or 10, and the mixtures were heated at 300 °C for 10 h in air. Then, reaction products were washed with water to remove any soluble component and dried in air at 80 °C. We denoted those Li^+-type samples as Li—the ratio of Li/K-Hollandite MnO_2. For example, Li-5-Hol indicated the Li^+ ion-exchanged product of the K-Hol sample in $LiNO_3$/LiCl with a ratio of Li/K = 5. Furthermore, α-$K_{0.14}MnO_2{\cdot}0.18H_2O$ (K-Hol) and α-$K_{0.14}(Mn_{0.85}Co_{0.15})O_2{\cdot}0.21H_2O$ (Co-K-Hol) samples were heat-treated at 300 °C for 2 h in air, and their dehydrated K^+-type samples (D-K-Hol and D-Co-K-Hol) were prepared. Then, the K^+ ions in these dehydrated samples were exchanged by Li^+ ions in $LiNO_3$/LiCl with a ratio of Li/K = 5 in a same way, and after washing with water and drying at 80 °C the Li^+-type samples (D-Li-Hol and D-Co-Li-Hol) were obtained.

The X-ray diffraction (XRD) measurements were performed using a Rigaku Rint 2200 diffractometer with a Cu Kα radiation. Atomic absorption spectroscopy (AAS) was employed to analyze the chemical compositions of the prepared powders. The water contents in the prepared powders were obtained from heating loss at 300 °C for 2 h in air. Manganese oxidation state was determined by an oxidation/reduction titration method using oxalic acid and $KMnO_4$. Scanning electron microscopy with energy dispersive X-ray spectrometer (SEM-EDX) and transmission electron microscopy (TEM) were performed to observe the morphology and analyse the composition of particles.

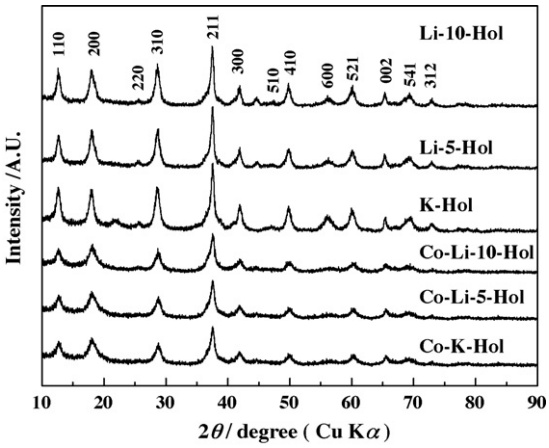

Fig. 1. Powder XRD patterns of α-$K_y(Mn_{1-x}Co_x)O_2{\cdot}zH_2O$ and their Li^+ ion-exchanged products.

For preparing electrodes, the prepared powders were mixed with acetylene black, graphite and polyvinyliden difluoride (PVDF) powder binder in a weight ratio of 70:10:10:10 in *N*-methyl-2-pyrrolidinone (NMP). After pasting the mixture on Ni-mesh, the electrodes were dried to remove NMP at 80 °C for 1 h in air, and then these electrodes were dried at 80 °C in vacuum for 24 h. The electrodes were tested in laboratory glass cells with lithium metal foil as a counter electrode and 1 M $LiClO_4$ in propylene carbonate (PC) as an electrolyte. The assembly of the cells was carried out in the Ar-filled glove box. The cells were discharged and charged at 25 °C with a current densities of 20–200 mA g^{-1} between the voltage limits of 4.0 and 2.0 V.

3. Results and discussion

3.1. Characterization of Li^+ ion-exchanged products of K^+-type hollandite MnO_2

Fig. 1 shows XRD patterns of the products from Li^+ ion-exchanging K^+-type α-MnO_2 and its Co-doped one. Table 1 shows the chemical compositions and unit cell parameters of the Li ion-exchanged products. The XRD patterns of the ion-exchanged products are considerably similar to those of parent K^+-type α-MnO_2 (K-Hol) and the Co-doped one (Co-K-Hol) prepared by a solution technique [11], suggesting that the

Table 1
Chemical compositions and unit cell parameters of α-$K_y(Mn_{1-x}Co_x)O_2{\cdot}zH_2O$ and their Li^+ ion-exchanged products

Sample	Composition	n in Mn^{n+}	a (Å)	c (Å)	V (Å^3)
K-Hol	$K_{0.14}MnO_{1.93}{\cdot}0.18H_2O$	3.73	9.77<u>5</u>	2.85<u>6</u>	272.<u>9</u>
Li-5-Hol	$(K_{0.01}Li_{0.42})MnO_{2.08}{\cdot}0.02H_2O$	3.72	9.88<u>8</u>	2.85<u>6</u>	279.<u>3</u>
Li-10-Hol	$(K_{0.01}Li_{0.37})MnO_{2.04}{\cdot}0.03H_2O$	3.70	9.84<u>3</u>	2.85<u>5</u>	276.<u>6</u>
K-Co-Hol	$K_{0.14}(Co_{0.15}Mn_{0.85})O_{1.96}{\cdot}0.21H_2O$	3.92	9.83<u>6</u>	2.85<u>8</u>	276.<u>5</u>
Li-5-Co-Hol	$(K_{0.04}Li_{0.34})(Co_{0.15}Mn_{0.85})O_{2.07}{\cdot}0.03H_2O$	3.90	9.95<u>7</u>	2.84<u>9</u>	282.<u>5</u>
Li-10-Co-Hol	$(K_{0.04}Li_{0.35})(Co_{0.15}Mn_{0.85})O_{2.08}{\cdot}0.03H_2O$	3.91	9.94<u>5</u>	2.85<u>2</u>	282.<u>1</u>

The underlined values show an accuracy.

original hollandite-structure is maintained through the Li^+ ion-exchange reaction in Li^+ ion-containing molten salt at 300 °C. All strong diffraction peaks of these samples can be indexed to the tetragonal phase (space group: *I4/m*). As seen in Table 1, almost all K^+ ions in the hollandite structure were exchanged by Li^+ ions in the molten salt and significantly large amounts of Li^+ ions were incorporated, leading to disappearance of the water molecules in the oxide structure through Li^+ ion-exchanging. The amounts of the oxygen in α-MnO_2 and its Co-doped were increased by Li^+ ion-exchanging, exceeding 2.0. Moreover, the mean Mn valence remained unchanged on Li^+ ion-exchanging. These facts indicate that the hydrogens in the water molecules were exchanged by Li^+ ions, resulting in a formation of Li_2O molecules. Thus, the amounts of Li^+ ions in the Li^+ ion-exchanged MnO_2 are close to the total amounts of K^+ ions and hydrogens of the water molecules approaching to $3Li/8(Mn_{1-x}Co_x)$ although a little amount of the water molecules were evaporated during the ion-exchange reaction at 300 °C. The Li-5-Hol and Li-5-Co-Hol samples can be expressed as $K_{0.01}{\cdot}Li_{0.13}{\cdot}(Li_2O)_{0.15}{\cdot}MnO_{1.93}$ and $K_{0.04}{\cdot}Li_{0.10}{\cdot}(Li_2O)_{0.12}{\cdot}(Mn_{0.85}Co_{0.15})O_{1.96}$, respectively. As seen in Table 1, the unit cells in α-MnO_2 and the Co-doped expand only to the direction of *a*-axis with Li^+ ion-exchanging, probably due to the incorporation of Li_2O molecules in (2 × 2) tunnels. Such a similar structural variation was also observed in the hollandite-type $xLi_2O{\cdot}MnO_2$ ($x = 0$–0.25) prepared by reaction of α-MnO_2 with $LiOH{\cdot}H_2O$ at 275 °C [9].

Fig. 2 gives the SEM-EDX images and TEM images of Li^+ ion-exchanged Co-doped MnO_2 (Li-5-Co-Hol) sample. The sample consisted of needle-like particles with the width of the needle ranging from 10 to 30 nm (Fig. 2b). The morphology of the other samples is similar to this sample. The SEM-EDX images show that the substituent of Co is well distributed in the particle, and K is scarcely observed in this sample.

Thus, the Li^+ ion-exchanging process can be schematically shown in Fig. 3. The K^+ ion and two hydrogens in water molecules in the large (2 × 2) tunnel in the hollandite-MnO_2 structure were exchanged with three Li^+ ions in molten salt at 300 °C, and one O^{2-} ion may occupy the center of the tunnel and three Li^+ ions may reside the (2 × 2) tunnel borders. On discharge, Li^+ ion insertion is possible through the remaining one (2 × 2) tunnel border site, and the existence of Li_2O in the tunnel may contribute to the structural stabilization for Li^+ ion insertion/deinsertion, as described by Johnson et al. [10].

Fig. 4 shows the XRD patterns of the dehydrated products of the K-Hol and Co-doped K-Co-Hol samples and their Li^+ ion-exchanged products. Table 2 shows the chemical composition and lattice parameters of the products. As seen in the Fig. 4, the XRD patterns of the dehydrated and ion-exchanged products are quite similar to the precursors K-Hol and K-Co-Hol, indicating that the original structures were maintained during dehydration and the following ion-exchanging. From Table 2, the most of the water molecules in the oxide was removed by heat-treating at 300 °C with keeping the original structure in both undoped K-Hol and Co-doped K-Co-Hol. Only the a-lattice parameter diminishes on dehydration, resulting in the decrease of the unit cell volume. Furthermore, K^+ ion in the dehydrated

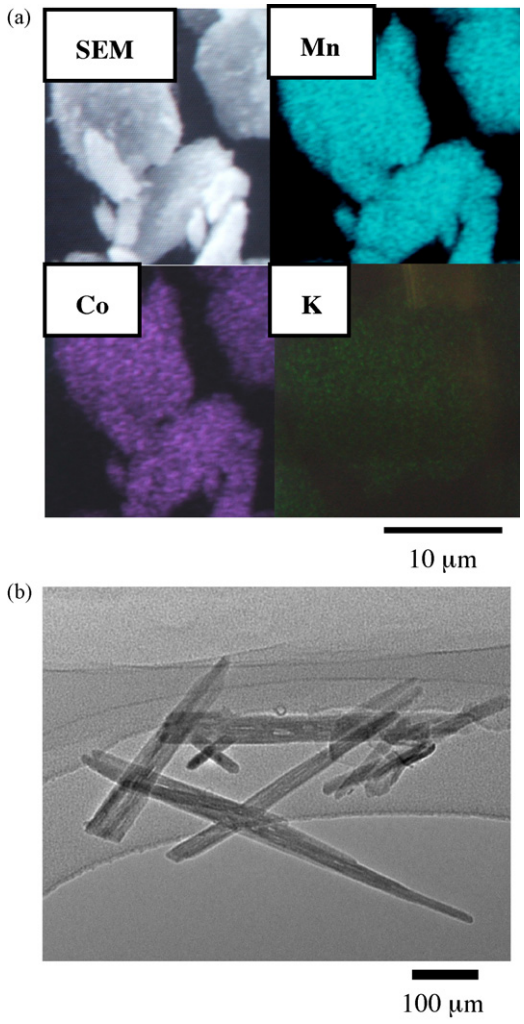

Fig. 2. SEM-EDX (a) and TEM (b) images of the Li-5-Co-Hol ($K_{0.04}Li_{0.34}(Mn_{0.85}Co_{0.15})O_{2.07}$) sample.

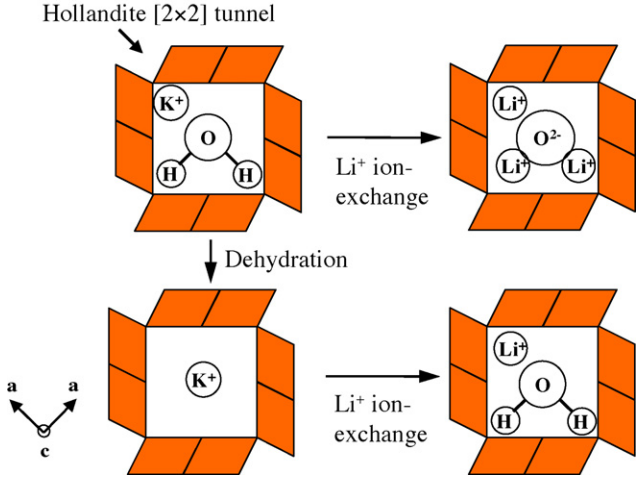

Fig. 3. Schematic drawing of hollandite-type MnO_2 in Li^+ ion-exchanging process and dehydration process.

Table 2
Chemical compositions and unit cell parameters of the products from dehydration and Li^+ ion-exchanging

Sample	Composition	n in Mn^{n+}	a (Å)	c (Å)	V (Å^3)
K-Hol	$K_{0.14}MnO_{1.93}\cdot 0.18H_2O$	3.73	9.77<u>5</u>	2.85<u>6</u>	272.<u>9</u>
D-K-Hol	$K_{0.14}MnO_{1.96}\cdot 0.02H_2O$	3.78	9.75<u>6</u>	2.85<u>6</u>	271.<u>8</u>
D-Li-Hol	$(K_{0.03}Li_{0.11})MnO_{1.91}\cdot 0.11H_2O$	3.68	9.81<u>2</u>	2.85<u>4</u>	274.<u>8</u>
K-Co-Hol	$K_{0.14}(Co_{0.15}Mn_{0.85})O_{1.96}\cdot 0.21H_2O$	3.92	9.83<u>6</u>	2.85<u>8</u>	276.<u>5</u>
D-K-Co-Hol	$K_{0.14}(Co_{0.15}Mn_{0.85})O_{1.98}\cdot 0.03H_2O$	3.97	9.79<u>6</u>	2.85<u>3</u>	273.<u>8</u>
D-Li-Co-Hol	$(K_{0.05}Li_{0.13})(Co_{0.15}Mn_{0.85})O_{1.99}\cdot 0.10H_2O$	3.94	9.81<u>0</u>	2.85<u>1</u>	274.<u>4</u>

The underlined values show an accuracy.

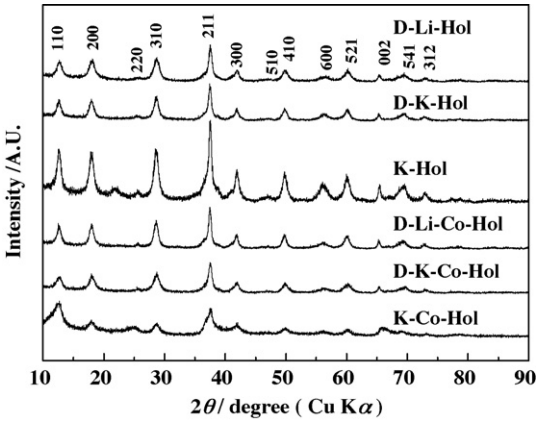

Fig. 4. Powder XRD patterns of α-$K_y(Mn_{1-x}Co_x)O_2\cdot zH_2O$ and their dehydrated and Li^+ ion-exchanged products.

D-K-Hol and D-Li-Co-Hol samples were mostly ion-exchanged by Li^+ in the molten salt with keeping the original structure in both undoped and Co-doped oxides, resulting in the formation of the Li^+-type α-MnO_2 (D-Li-Hol and D-Li-Co-Hol) not including Li_2O molecules in the (2×2) tunnels. However, the water molecules were incorporated during washing the Li^+ ion-exchanged products with water, leading to the increase in the a-lattice parameter in both D-Li-Hol and D-Li-Co-Hol samples. Thus, the dehydration and Li^+ ion-exchanging processes can be shown schematically in Fig. 3.

3.2. Lithium insertion properties of Li^+ ion-exchanged hollandite MnO_2

Electrochemical investigations including charge–discharge cyclings were carried out for α-$K_y(Mn_{1-x}Co_x)O_2$ and their Li^+ ion-exchanged and dehydrated MnO_2 electrodes. Figs. 5 and 6 show initial discharge and cyclic curves of α-MnO_2 and its Co-doped one at a current density of 20 mA g^{-1} and 25 °C, respectively. Table 3 summarizes the electrochemical performances of α-MnO_2 and its Co-doped electrodes. As seen in the initial discharge curves, a smooth voltage variation consisting of one-step is observed in any electrode, suggesting that a single-phase formation reaction occurs during discharge. The initial discharge capacity for the K-Hol sample is 141 mAh g^{-1} corresponding to 0.46 mol Li insertion per formula unit, and that for the Co-doped K-Co-Hol sample is 171 mAh g^{-1} (0.60 Li/(Mn + Co)) higher than that for the K-Hol sample. The discharge capacities of the K-Hol and Co-K-Hol samples are

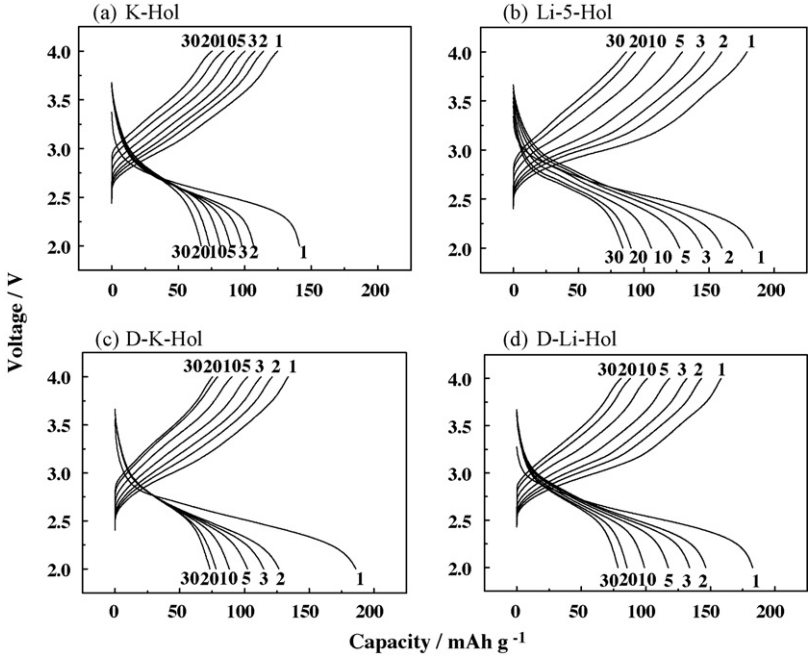

Fig. 5. Charge–discharge curves of (a) K-Hol, (b) Li-5-Hol, (c) D-K-Hol, and (d) D-Li-Hol.

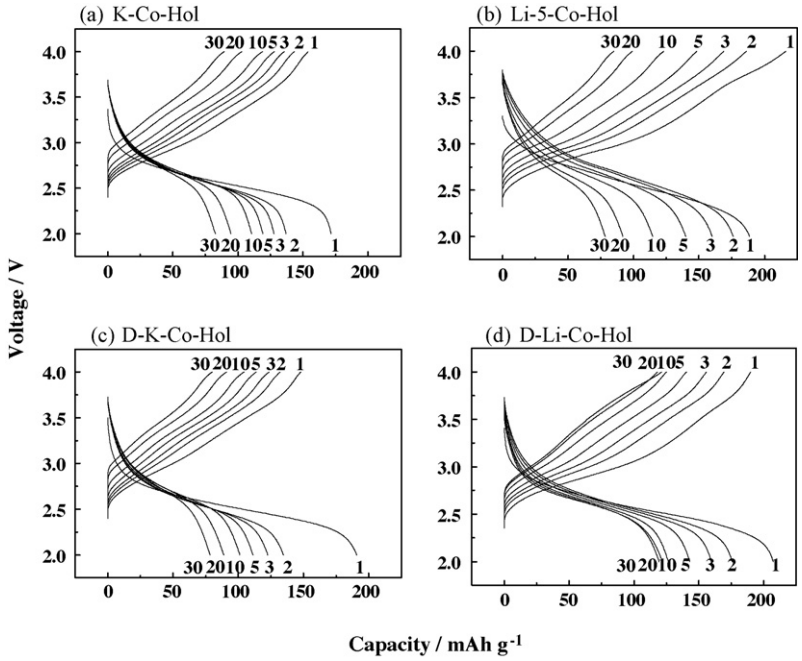

Fig. 6. Charge–discharge curves of (a) K-Co-Hol, (b) Li-5-Co-Hol, (c) D-K-Co-Hol, and (d) D-Li-Co-Hol.

increased by Li^+ ion-exchanging to 181–188 mAh g^{-1} corresponding to about 0.60 Li/(Mn + Co). The recharge efficiencies of the K-Hol and its Co-doped K-Co-Ho samples are 87–90%, which were enhanced to almost 100% with Li^+ ion-exchanging. However, it should be noticed that in the cases of the Co-doped Li-5-Co-Hol and Li-10-Co-Hol samples the efficiency exceeds 100%, reaching 111–114%. This may be due to the oxidation reaction of Co^{3+} to Co^{4+} ion during recharge at the potential of 3.8–4.0 V, where a voltage plateau appears as is the case of $LiCoO_2$ [13]. Furthermore, their discharge capacities decreased gradually with increasing cycling number as seen in Figs. 5 and 6. At the 10th cycle, the Li^+ ion-exchanged samples show the capacities of 113–116 mAh g^{-1}, which are higher than those for the precursors (K-Hol and Co-K-Hol).

As shown in Fig. 3, in the cases of the Li^+ ion-exchanged samples, such as the Li-5-Hol and Li-5-Co-Hol, Li_2O molecules may occupy the (2 × 2) tunnel and Li^+ ions can be incorporated into the vacant site of the (2 × 2) tunnel border on discharge. Therefore, such an enhanced electrochemical performance by Li^+ ions-exchanging may be caused by a structural stabilization with the existence of Li_2O in the (2 × 2) tunnel.

The D-K-Hol sample from dehydration of the precursor K-Hol shows the discharge capacity of 186 mAh g^{-1}, corresponding to that of Li_2O-containing Li-5-Hol and Li-10-Hol samples in spite of increased amount of the structural vacancy in the (2 × 2) tunnel with dehydration. On the other hand, in the Co-doped D-K-Co-Hol sample from dehydration of the precursor K-Co-Hol a higher discharge capacity of 191 mAh g^{-1} (0.62 Li/(Mn + Co)) was obtained, probably due to the structural stabilization with Co-doping [11]. However, these dehydrated samples show considerably lower recharge efficiency of 72–75%, leading to a lower cycling capacity at the 10th cycle. This would be due to the deterioration of the crystal lattice arrangement with Li^+ ion insertion. Moreover, in the Co-doped D-Li-Co-Hol sample from Li^+ ion-exchange of the D-K-Co-Hol sample, high discharge capacities of 207 and 126 mAh g^{-1} at initial and the 10th cycle were obtained probably due to the structural stabilization with water molecules together with a small amount of K^+ ions in the (2 × 2) tunnel as shown in Fig. 3.

Fig. 7 represents the initial discharge curves and cycle performances of the Li-5-Co-Hol sample at various current densities. As seen in the figure, 86 and 93% of the discharge capacities at 20 mA g^{-1} were maintained even at a high current density of 100 mA g^{-1} at the initial (Fig. 7a) and 10th cycle (Fig. 7b), respectively.

The structural variation in the Li-5-Hol and Li-5-Co-Hol samples during 30 cyclings was examined by ex-situ XRD measurements. It was observed that the crystal lattice of the

Table 3
Electrochemical performances of α-$K_y(Mn_{1-x}Co_x)O_2 \cdot zH_2O$ and their Li^+ ion-exchanged and dehydrated products

Sample	Initial discharge		Recharge (%)	10th Cycle (mAh g^{-1})
	Capacity (mAh g^{-1})	Li/(Mn + Co)		
K-Hol	141	0.46	87	81
Li-5-Hol	183	0.59	98	113
Li-10-Hol	186	0.60	100	113
D-K-Hol	186	0.60	72	88
D-Li-Hol	183	0.59	86	99
K-Co-Hol	171	0.56	90	111
Li-5-Co-Hol	188	0.61	114	115
Li-10-Co-Hol	181	0.59	111	116
D-K-Co-Hol	191	0.62	75	101
D-Li-Co-Hol	207	0.67	92	126

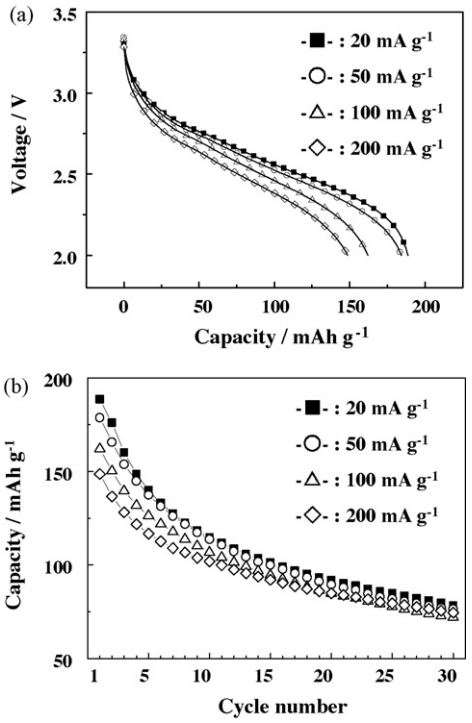

Fig. 7. Discharge curves (a) and cycle performances (b) of Li-5-Co-Hol sample at various current densities.

samples disordered gradually with discharge while keeping the original crystal lattice, followed by further disordering with increased cyclings. Thus, the considerable decrease in capacity with cyclings may be caused by increasing structural disordering as well as increasing diffusion polarization of Li^+ ions during charging.

4. Conclusions

The Li^+-type α-MnO_2 and its Co-doped one were prepared by ion-exchanging the K^+-type α-$K_{0.14}MnO_{1.93}\cdot 0.18H_2O$ and its Co-doped α-$K_{0.14}(Mn_{0.85}Co_{0.15})O_{1.96}\cdot 0.21H_2O$ with Li^+ ions in a $LiNO_3$/LiCl molten salt at 300 °C. Almost all the K^+ ions and hydrogens in water in the (2×2) large tunnels were exchanged by Li^+ ions in the molten salt, leading to $K_{0.14-y}Li_y\cdot(Li_2O)z\cdot Mn_{1-x}Co_xO_{2+\delta}$ ($y=0.10$–0.13, $z=0.12$–0.15), where both the Li^+ ions and Li_2O are incorporated in the (2×2) tunnel. Furthermore, the anhydrous α-$K_{0.14}(Mn_{1-x}Co_x)O_2$ samples obtained from dehydration of the K^+-type precursors were also ion-exchanged by Li^+ ions in the molten salt at 300 °C, leading to the Li^+ ion-type α-MnO_2 not including Li_2O in the structure. XRD measurement showed that the hollandite structure of K^+-type precursors was maintained through Li^+ ion-exchanging. The Li^+ ion-exchanged samples are needle-like crystals with the width of 10–30 nm.

The electrochemical measurements indicated that the Li^+ ion-exchanged α-MnO_2 and its Co-doped electrodes showed 181–207 mAh g^{-1} corresponding to 0.59–0.67 Li/(Mn + Co) at the initial discharge, and 113–126 mAh g^{-1} at the 10th cycle, which are superior to the K^+-type precursors. The Li^+ ion-exchanged products show excellent rate performance, but the discharge capacity decreases with increasing cycling number because of increasing structural disordering. Thus, further study will be done for improving the cycling performance, e.g., by an increase in the structural stability from ion-exchanging the precursor with large cations, such as Na^+, K^+, and Rb^+.

Acknowledgements

We would like to thank Ms. Yuko Mitobe in Iwate University for the helpful assistance in the experimental work. This study was partially supported by Japan and Grant-in-Aid for Scientific Research (B) from Japan Society for the Promotion of Science (JSPS).

References

[1] J.M. Tarascon, E. Wang, F.K. Shocoohi, W.R. Mckinnon, S. Colson, J. Electrochem. Soc. 138 (1991) 2859.
[2] L. Guohua, H. Ikuta, T. Uchida, M. Wakihara, J. Electrochem. Soc. 143 (1996) 178.
[3] N. Kumagai, T. Fujiwara, K. Tanno, T. Horiba, J. Electrochem. Soc. 143 (1996) 1007.
[4] W.F. Cole, A.D. Wadsley, A. Nalkley, Trans. Electrochem. Soc. 92 (1947) 133.
[5] K.M. Parida, S.B. Kanungo, B.R. Sant, Electrochim. Acta 26 (1981) 435.
[6] M. Tsuji, M. Abe, Solvent Extr. Ion Exc. 2 (1984) 253.
[7] Q. Feng, H. Kanoh, K. Ooi, M. Tani, Y. Nakacho, J. Electrochem. Soc. 141 (1994) L135.
[8] Ph. Botkovitz, Ph. Deniard, M. Tournoux, R. Brec, J. Power Sources 43/44 (1993) 657.
[9] C.S. Johnson, D.W. Dees, M.F. Mansuetto, M.M. Thackeray, D.R. Vissers, D. Argyriou, C.-K. Loong, L. Christensen, J. Power Sources 68 (1997) 570.
[10] C.S. Johnson, M.F. Mansuetto, M.M. Thackeray, Y. Shao-Horn, S.A. Hackney, J. Electrochem. Soc. 144 (1997) 2279.
[11] T. Sasaki, S. Komaba, N. Kumagai, I. Nakai, Electrochem. Solid-State Lett. 8 (2005) A471.
[12] N. Kumagai, S. Oshitari, S. Komaba, J. New Mater. Electrochem. Syst. 9 (2006) 175.
[13] S.-T. Myung, N. Kumagai, S. Komaba, H.-T. Chung, J. Appl. Electrochem. 30 (2000) 1081.